Problem statement

Identify the cut-off frequency and design a 7th order filter FIR using three different windows:

1. Rectangular window-

   WR = 1; $0 \leq n \leq M - 1$

2. Hamming Window-

   $Wh(n) = 0.54 - 0.46 * \cos[2\pi n/(M - 1)]$; $0 \leq n \leq M - 1$

3. Hanning Window-

   $Whan(n) = 0.5 - 0.5 * \cos[2\pi n/(M - 1)]$; $0 \leq n \leq M - 1$

Background calculation

$$h(n) = \frac{1}{2\pi}\left[\int_{-\pi}^{-3\pi/4} e^{-j3w} e^{jwn}\, dw + \int_{3\pi/4}^{\pi} e^{-j3w} e^{jwn}\, dw\right]$$

$$= \frac{1}{\pi(n-3)} \left[-\sin \frac{3\pi}{4}(n-3) \right.$$

It can be concluded that we can use this h(n) equation to determine the filter operation in different windows. We will be taking the cutoff frequency at 3pi/4 for default window technique.

Rectangular window

Rectangular window :

$h(n)$	$W_{rect}(n)$	$h'(n)$
-0.075	1	-0.075
0.159	1	0.159
-0.225	1	-0.225
0.25	1	0.25

$h'(n) = \{-0.075, 0.159, -0.225, 0.25, -0.225, 0.159, -0.075\}$

$\therefore H(w) = -0.075 + 0.159e^{-jw} - 0.225e^{-2jw} + 0.25e^{-3jw} - 0.225e^{-4jw} + 0.159e^{-5jw} - 0.075e^{-6jw}$

Code with theoretical values

```
w = 0: 0.001: 2*pi;

Hrec = -0.075*exp(-j*w*0) + 0.159*exp(-j*w*1) - 0.225*exp(-j*w*2)
+0.25*exp(-j*w*3) - 0.225*exp(-j*w*4) + 0.159*exp(-j*w*5) -
0.075*exp(-j*w*6);

phrec = angle(Hrec);

subplot(311), plot(w,Hrec), title('Rectangular Window magnitude
spectrum')
subplot(311), plot(w,phrec), title('Rectangular Window Phase
spectrum')
```

Output

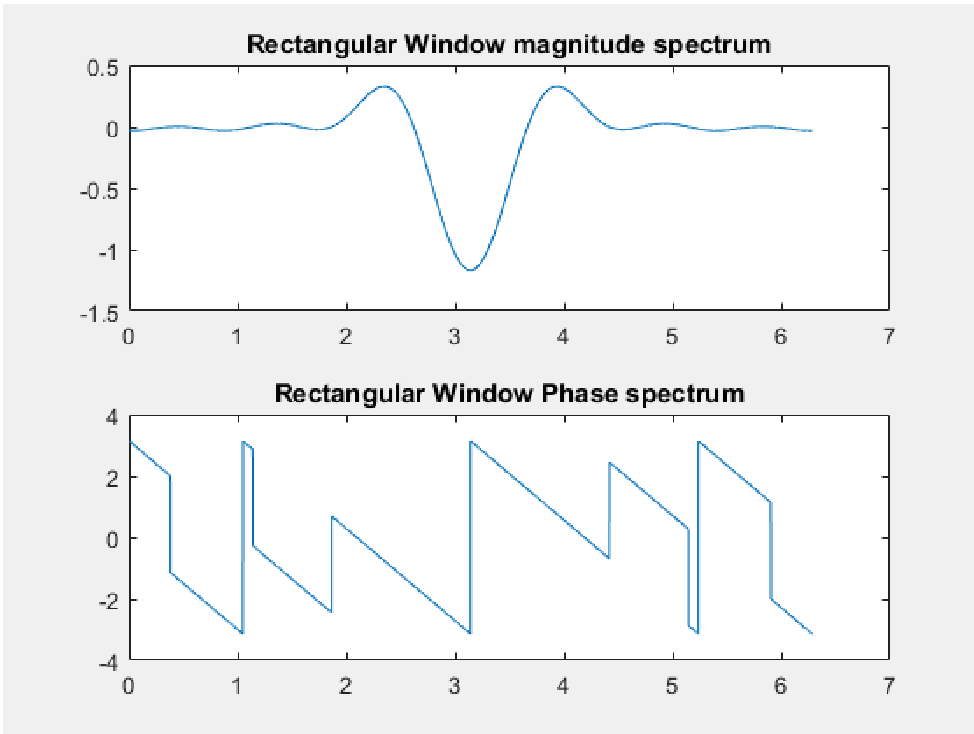

Fig.1: Rect window phase and mag. spectra(calculated)

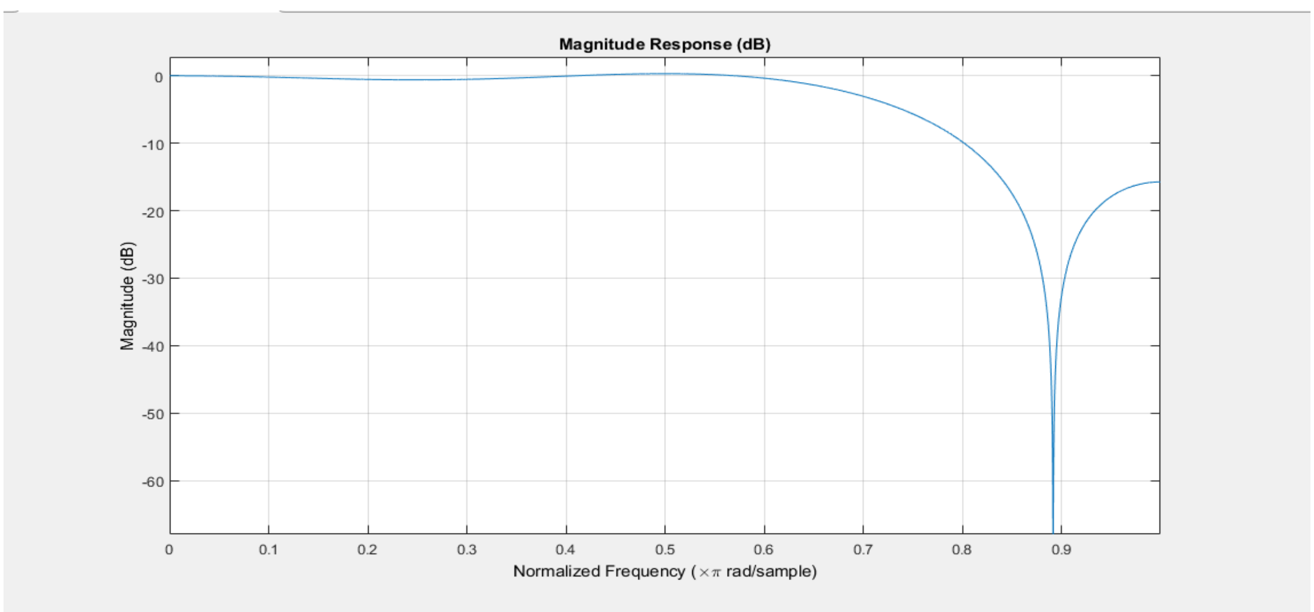

Fig.2: Rect window mag. spectrum (default function)

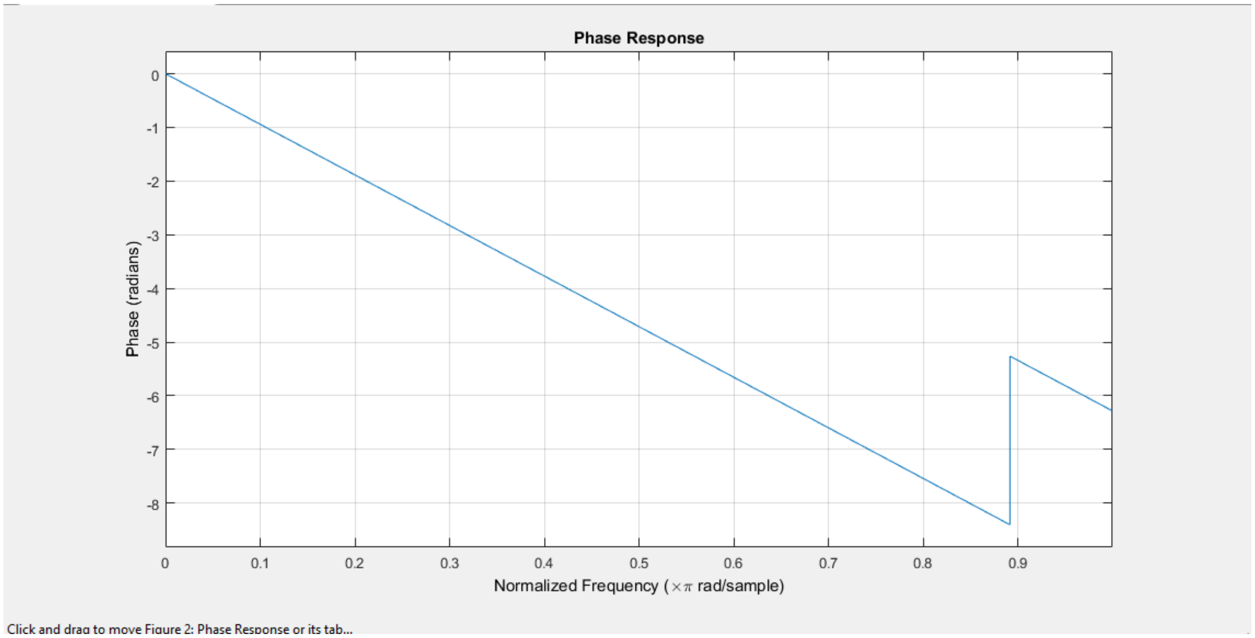

Fig.3: Rect window phase spectrum (default function)

Comparing the magnitude spectrum of the calculated output and default output of the rectangular window we can see that it is somewhat close to each other. Subsequently, the phase response in fig.1 has the first lowest point at n~=1.1 whereas the phase response in fig.3 has the first lowest point at n=0.9. This also can be drawn out to be somewhat close.

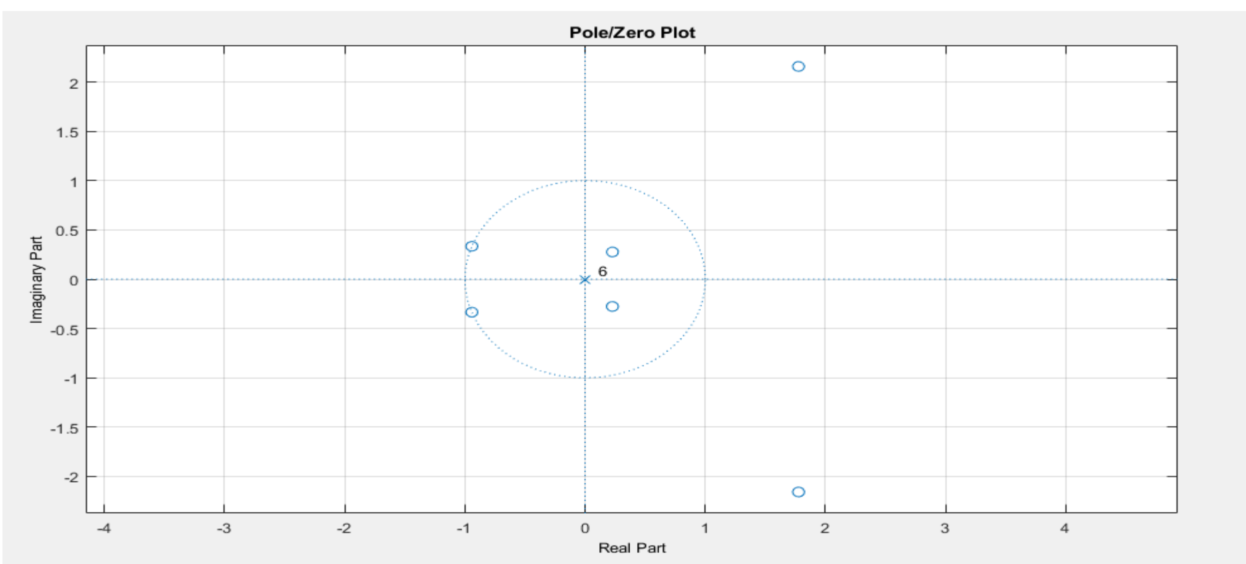

Fig.4: Pole/zero plot of rect window (default)

Analyzing fig.4, we can say that as the pole is located on the zero point, and thus it is marginally stable.

```
Numerator:
 0.072706936339467954
-0.15423470317480928
 0.21812080901840394
 0.72681391563387476
 0.21812080901840394
-0.15423470317480928
 0.072706936339467954
```

Fig.5: Filter coefficients (default)

Comparing the default generated filter coefficients with the calculated coefficients we can see that the absolute coefficients match with each other to the hundredth decimal value except for n=3.

Hanning window

Hanning window:

$$h(n) = \frac{1}{\pi(n-3)}\left[-\sin\frac{3\pi}{4}(n-3)\right] \qquad \Big|\ M-1=6$$

for $n = 3$,

$$\int_{-\pi}^{-3\pi/4} e^{j\omega 3} e^{j\omega -3}\, d\omega \qquad \Bigg| \qquad \int_{3\pi/4}^{\pi} e^{j\omega 3} e^{j\omega -3}\, d\omega$$

$$= \left[-\frac{3\pi}{4} + \pi\right] \qquad \Bigg| \qquad = \left[\pi - \frac{3\pi}{4}\right]$$

$$\therefore h(3) = \frac{1}{2\pi}\left[\frac{\pi}{4} + \frac{\pi}{4}\right] = \frac{1}{2\pi} \times \frac{2\pi}{4} = \frac{1}{4} = 0.25$$

	$h(n)$	$w_{han}(n)$	$h'(n) = h(n) * w_{han}(n)$
$n=0$	0.075	0	0
$n=1$	-0.159	0.25	-0.039
$n=2$	0.225	0.75	0.168
$n=3$	0.25	1	0.25

We get infinite value at this point for $n=3$

$$\therefore h'(n) = \{ \underset{\uparrow}{0}, -0.039, 0.168, 0.25, 0.168, -0.039, 0 \}$$

$$H(\omega) = \sum_{n=0}^{6} h'(n)\, e^{-j\omega n}$$

$$= 0 \cdot e^{-j\omega 0} - 0.039\, e^{-j\omega} + 0.168\, e^{-2j\omega} + 0.25\, e^{-3j\omega} + 0.168\, e^{-4j\omega} - 0.039\, e^{-5j\omega} + 0 \cdot e^{-j\omega 6}$$

Code with theoretical values

```
w = 0: 0.001: 2*pi;

Hhan = 0*exp(-j*w*0) - 0.039*exp(-j*w*1) + 0.168*exp(-j*w*2) +
0.25*exp(-j*w*3) + 0.168*exp(-j*w*4) - 0.039*exp(-j*w*5) +
0*exp(-j*w*6);


phhan = angle(Hhan);

 subplot(211), plot(w,Hhan), title('Hanning Window magnitude
spectrum')


subplot(212), plot(w,phhan), title('Hanning Window Phase spectrum')
```

Output

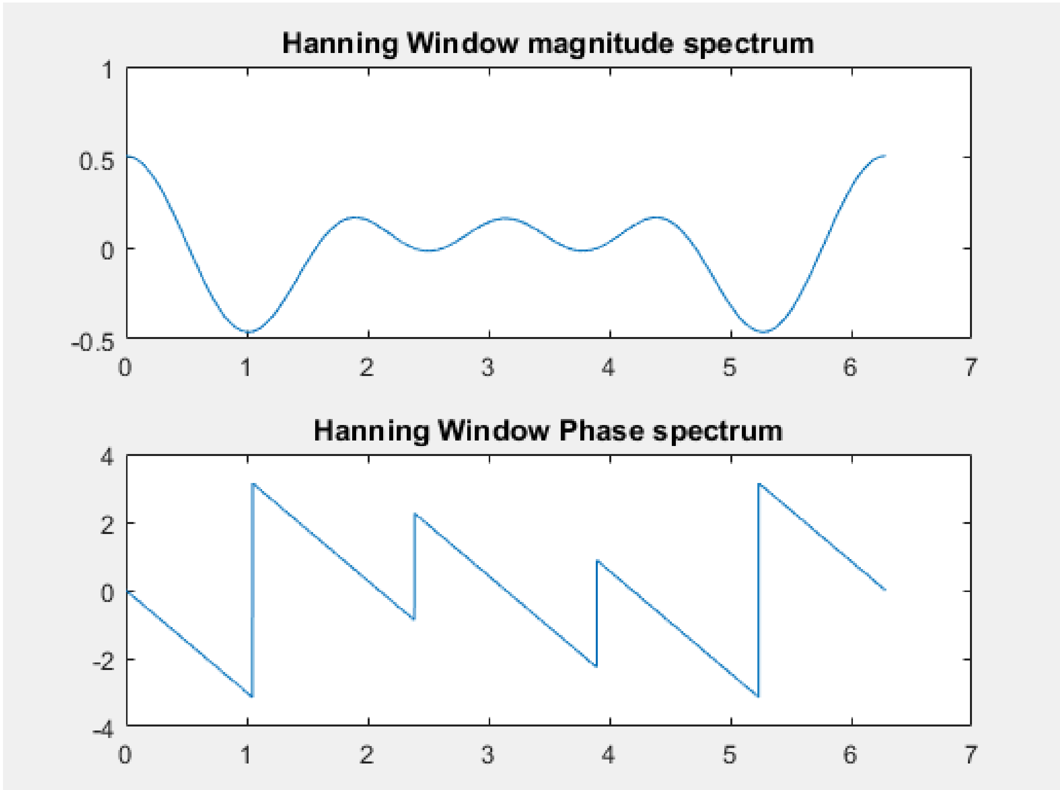

Fig.6: Hanning window phase and mag. spectra(calculated)

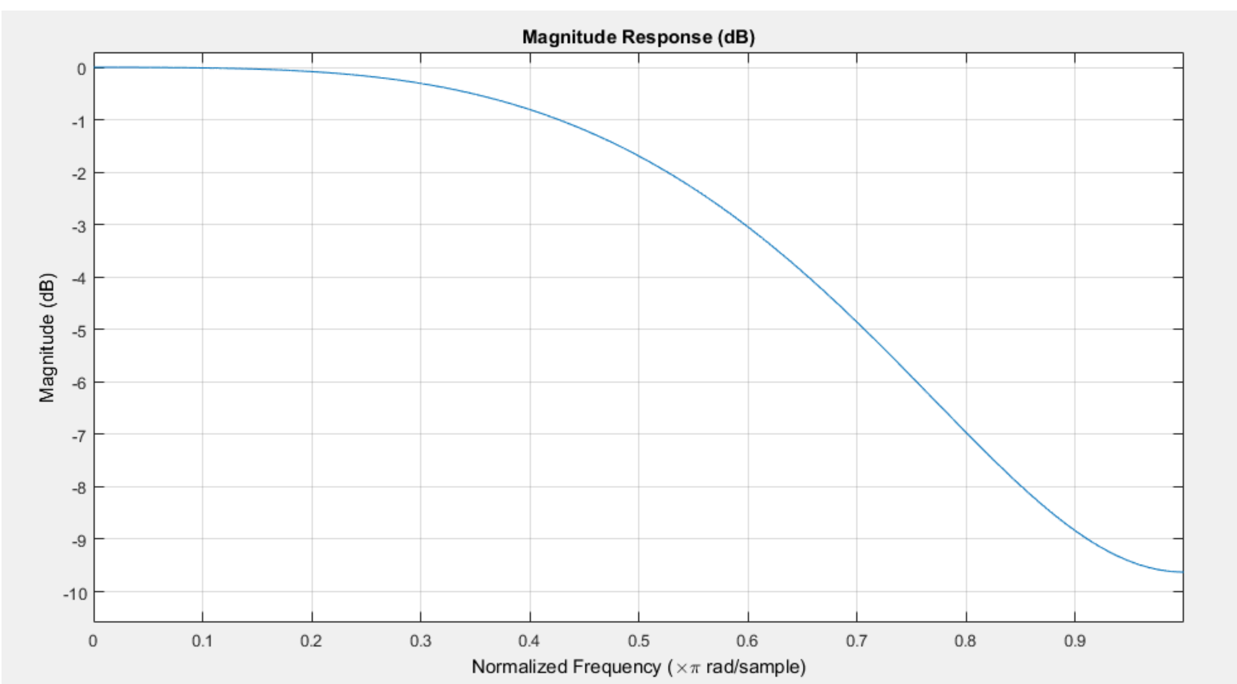

Fig.7: Hanning window mag. spectrum (default function)

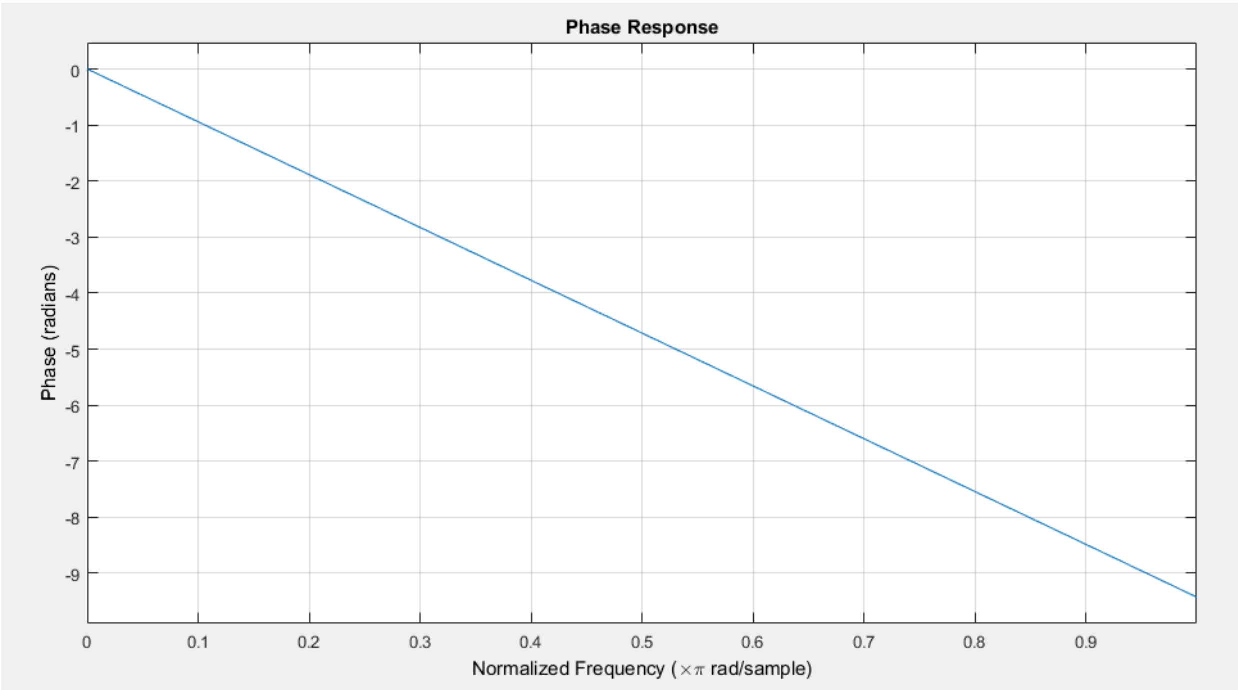

Fig.8: Hanning window phase spectrum (default function)

Comparing the magnitude spectrum of the calculated output and default output of the Hanning window we can see that it is moderately close to each other. Subsequently, the phase response in fig.6 has the first lowest point at n=1 whereas the phase response in fig.8 has the first lowest point at n~= 1. This also can be drawn out to be moderately close.

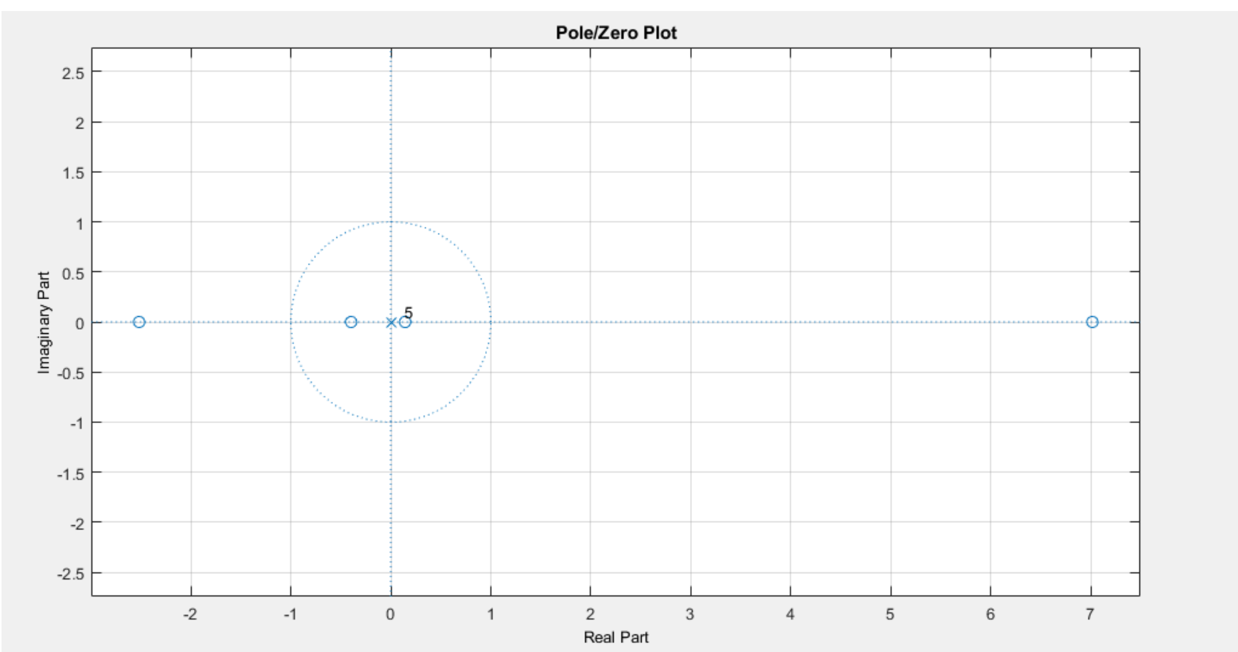

Fig.9: Pole/zero plot of Hanning window (default)

Analyzing fig.9, we can say that as the pole is located on the zero point, and thus it is marginally stable.

```
Numerator:
 0
-0.039471340917854418
 0.16746271695324544
 0.74401724792921797
 0.16746271695324544
-0.039471340917854418
 0
```

Fig.10: Filter coefficients (default)

Comparing the default generated filter coefficients with the calculated coefficients we can see that the absolute coefficients match with each other to the hundredth decimal value except for n=3.

Hamming window

Hamming window

	$h(n)$	$W_{hum}(n)$	$h'(n)$
$n=0$	-0.075	0.08	-0.006
$n=1$	0.159	0.031	0.0049
$n=2$	-0.225	0.77	0.12325
$n=3$	0.25	1	0.25

infinity value

$h'(n) = \{-0.006, 0.049, 0.1732, 0.2…, 0.1732, 0.049, -0.006\}$

$\therefore H(\omega) = -0.006 + 0.049e^{-j\omega} + 0.1732e^{-2j\omega} + 0.25e^{-3j\omega} + 0.1732e^{-4j\omega} + 0.049e^{-5j\omega} - 0.006e^{-6j\omega}$

Code with theoretical values

```
w = 0: 0.001: 2*pi;

Hham = -0.006*exp(-j*w*0) + 0.049*exp(-j*w*1) + 0.1732*exp(-j*w*2) +
0.25*exp(-j*w*3) + 0.1732*exp(-j*w*4) +0.049*exp(-j*w*5)
-0.006*exp(-j*w*6);



phham = angle(Hham);

subplot(211), plot(w,Hham), title('Hamming Window magnitude
spectrum')
subplot(212), plot(w,phham), title('Hamming Window Phase spectrum')
```

Output

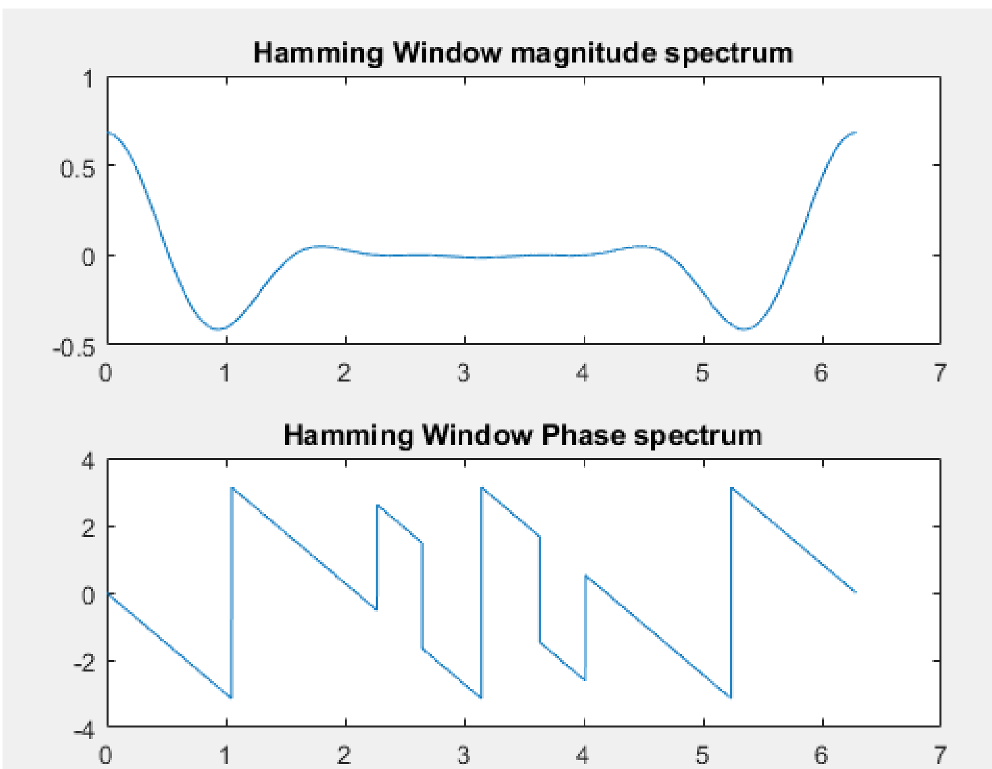

Fig.11: Hamming window phase and mag. spectra(calculated)

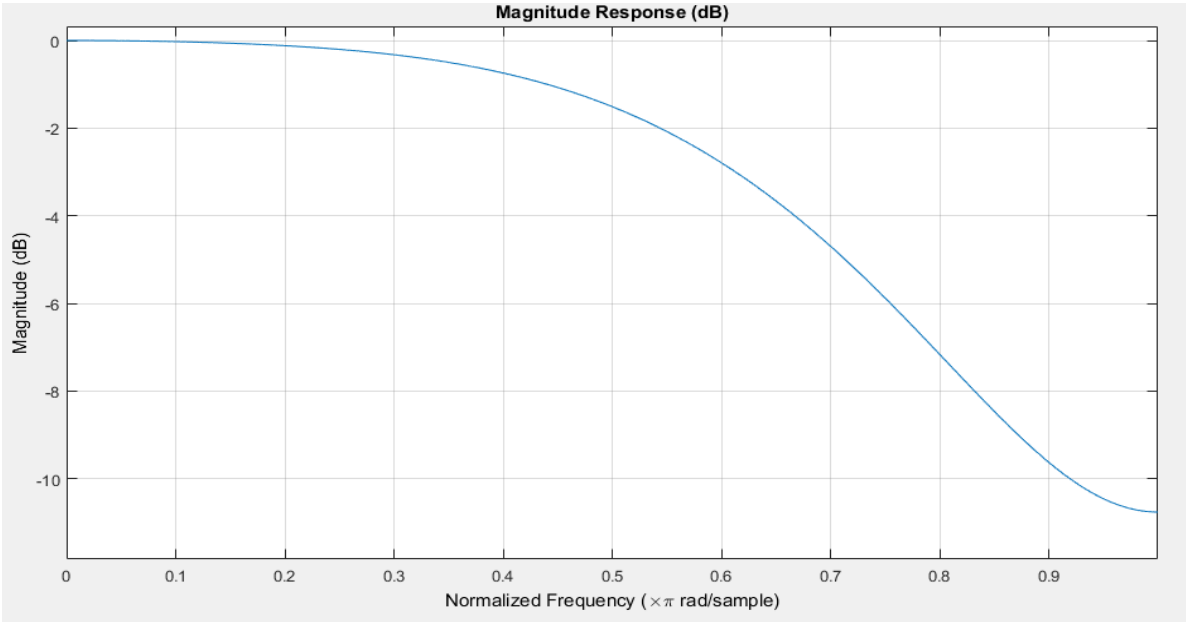

Fig.12: Hamming window mag. spectrum (default function)

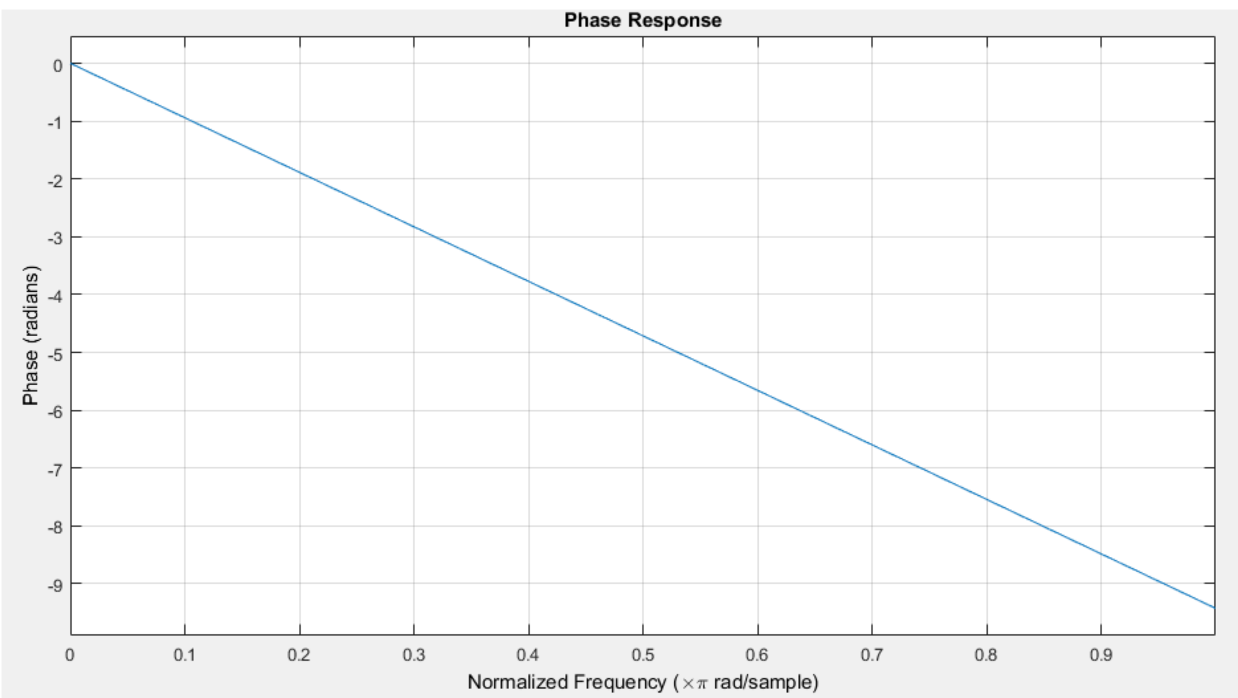

Fig.13: Hamming window phase spectrum (default function)

Comparing the magnitude spectrum of the calculated output and default output of the Hamming window we can see that they are very close to each other. Subsequently, the phase response in fig.10 has the first lowest point at n~=1 whereas the phase response in fig.8 has the first lowest point at n~= 1. This also can be drawn out to be very close.

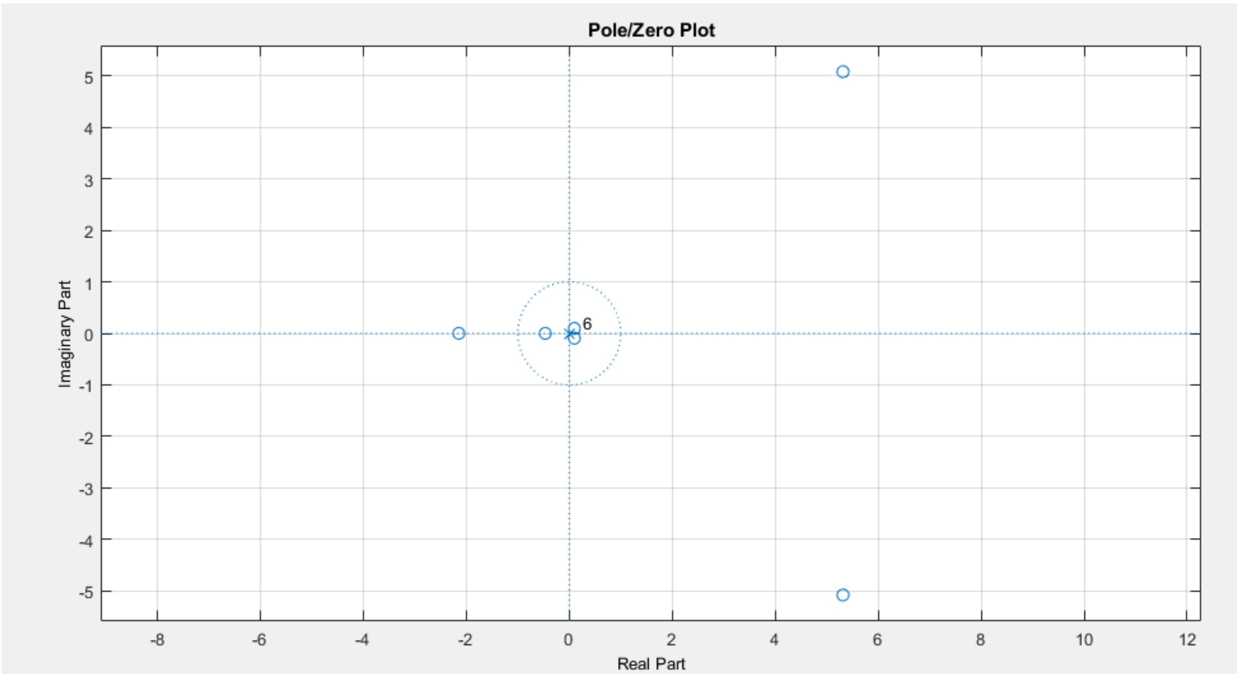

Fig.14: Pole/zero plot of Hamming window (default)

Analyzing fig.14, we can say that as the pole is located on the zero point, and thus it is marginally stable.

```
Numerator:
 0.005942976546695399
-0.048851958567985777
 0.1716034477858296 7
 0.742611068470921 4
 0.1716034477858296 7
-0.048851958567985777
 0.005942976546695399
```

Fig.15: Filter coefficients (default)

Comparing the default generated filter coefficients with the calculated coefficients we can see that the absolute coefficients match with each other to the thousandth decimal value except for n=3.

Comparative Analysis

Spectra

Due to the magnitude spectrum being in db scale in the default window, it is easier to compare the phase spectrum values. But the hamming window showcases much more linear output in $0<n<7$ range than the other two. Following this, among the 3 windows, in the parameter of first lowest point of respective phase spectra, the hamming and hanning window showcased closer to the calculated spectrum value compared to the rectangular window. Moreover, the hamming window showcased a slightly steep drop off than hanning and thus it is chosen as the winner here.

Stability

Analyzing the pole/zero plot of the default functions, it is evident that all three of them are in marginally stable/critically unstable condition.

Filter coefficients

The filter coefficients have been the most tricky part in this assignment. We can easily conclude from the comparison that is given in three of the sections that the filter coefficients match with the theoretically calculated values mostly except for n=3. Here, n=3 is the value which is responsible for the symmetrical condition. My theory is that due to the limited knowledge of default functions, I should have used a different construction of the default function when dealing with this assignment. However, given the results at hand, again as the hamming window boasts matched coefficients up to the thousandths decimal place, it can be called winner.

Discussion and Conclusion

This assignment challenged our critical thinking skills and ability to generate solutions from out of the box thinking. Although I could not completely verify my calculations with inbuilt matlab functions, it is sufficient to say that the results are conclusive enough to draw an argument to the hamming window's victory.

Find the matlab files : [EEE343 Design assignment - Google Drive]

Matlab

Rectangular Window:

Magnitude Spectrum:

Code:

```
clc
clear all
close all

w = 0: 0.001: 2*pi;
H_rec = -0.075*exp(-j*w*0) + 0.159*exp(-j*w*1) - 0.225*exp(-j*w*2) +
0.25*exp(-j*w*3) - 0.225*exp(-j*w*4) + 0.159*exp(-j*w*5) -
0.075*exp(-j*w*6); %calculated H(w) of rect window

H_rec = abs(H_rec); %calculates magnitude
plot(w,H_rec), title('Rectangular Window magnitude spectrum'),
xlabel('w'),ylabel('|H(w)|')
```

Output:

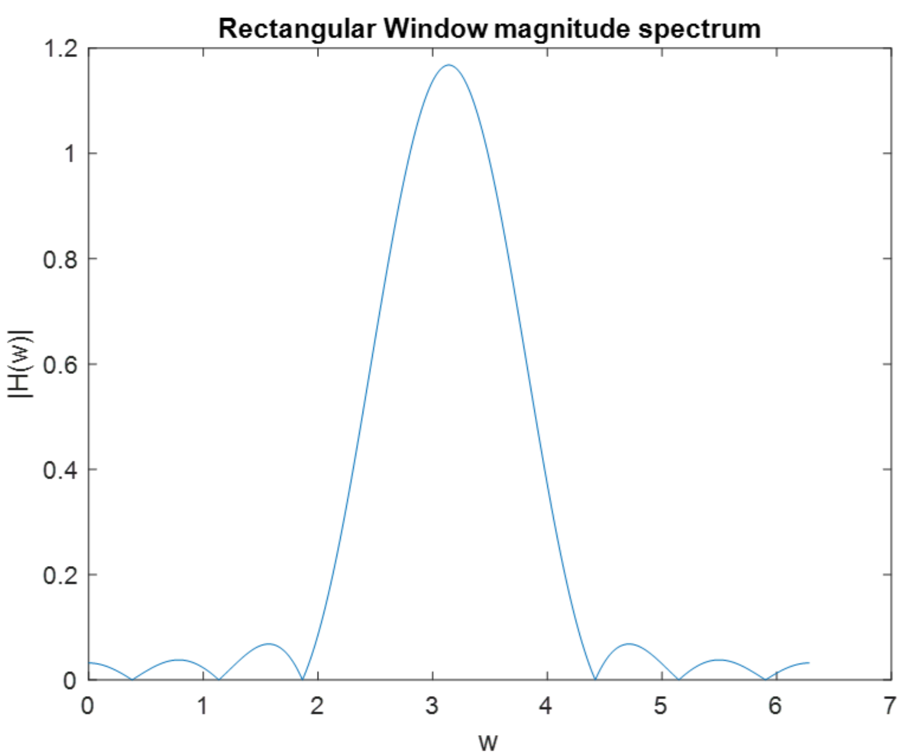

Fig 1: Magnitude Spectrum with Calculated values

Phase Spectrum:

Code:
```
clc
clear all
close all

w = 0: 0.001: 2*pi;
H_rec = -0.075*exp(-j*w*0) + 0.159*exp(-j*w*1) - 0.225*exp(-j*w*2) +
0.25*exp(-j*w*3) - 0.225*exp(-j*w*4) + 0.159*exp(-j*w*5) -
0.075*exp(-j*w*6);%calculated H(w) of rect window

ph_rec = angle(H_rec); %calculates phase
plot(w,ph_rec), title('Rectangular Window Phase spectrum'),
xlabel('w'),ylabel('<H(w)')
```

Output:

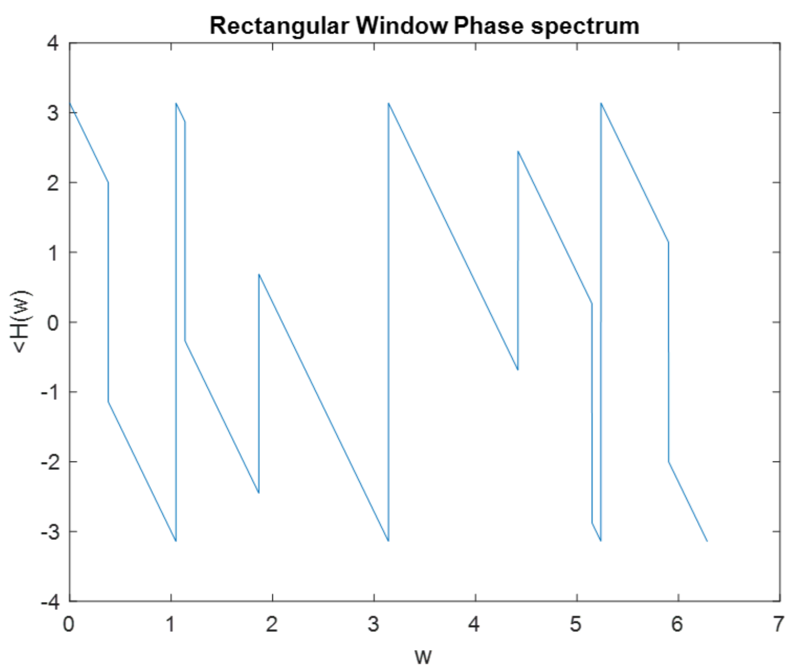

Fig 2: Phase Spectrum with Calculated values

Default Function:

Code:
```
clc
clear all
close all
```

```
a_rec = -fir1(6, 3/4, rectwin(7))%finds h'(n) coefficients
fvtool(a_rec) %plots magnitude spectrum
```

Output:

```
Command Window

a_rec =

   -0.0727    0.1542   -0.2181   -0.7268   -0.2181    0.1542   -0.0727

fx >>
```

Fig 3: H’(n) coefficients with default matlab function

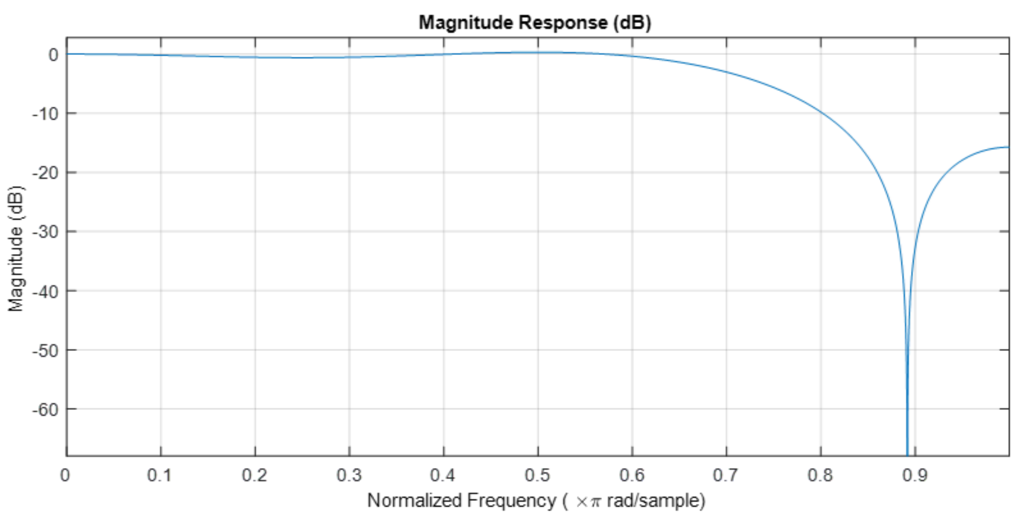

Fig 4: Magnitude Spectrum with default matlab function

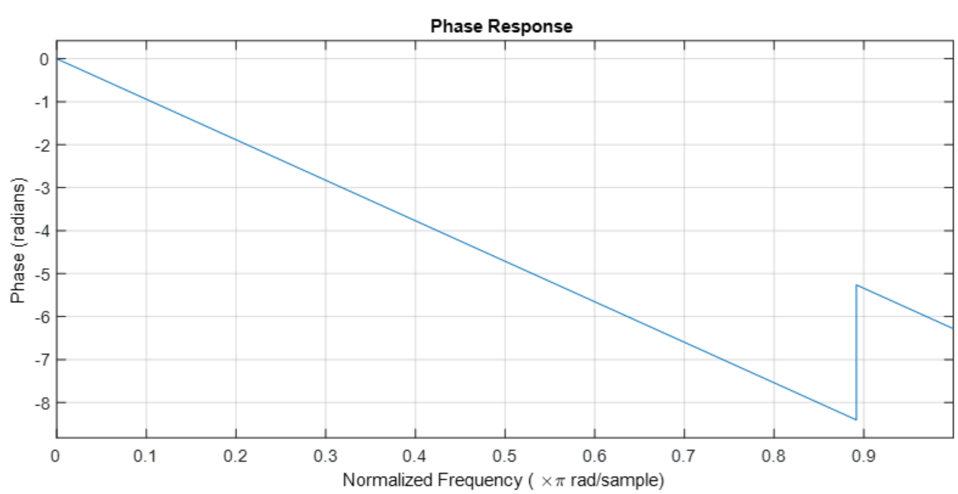

Fig 5: Phase Spectrum with default matlab function

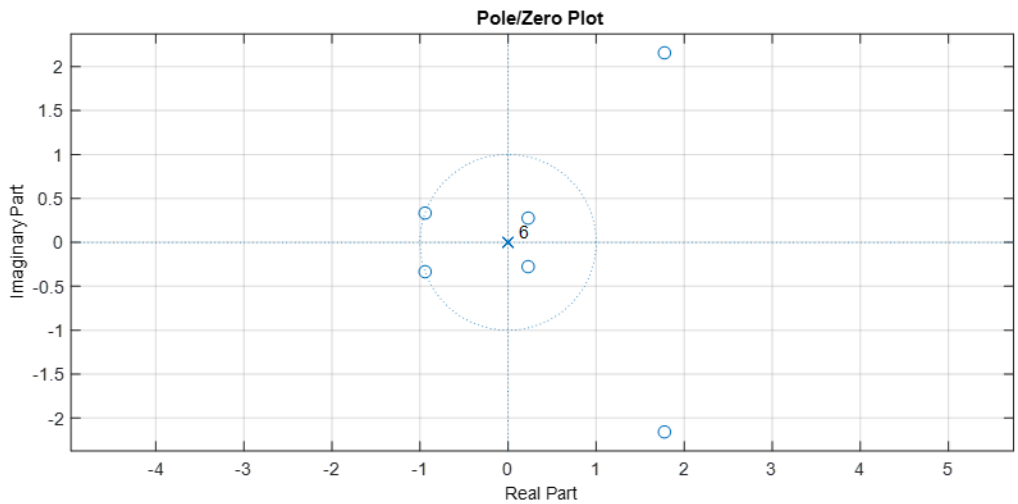

Fig 6: Pole-zero plot with default matlab function

Hamming Window:

Magnitude Spectrum:

Code:

```
clc
clear all
close all

w = 0: 0.001: 2*pi;
H_ham = -0.006*exp(-j*w*0) + 0.04929*exp(-j*w*1) +
0.17325*exp(-j*w*2) + 0.25*exp(-j*w*3) + 0.17325*exp(-j*w*4)
+0.04929*exp(-j*w*5) -0.006*exp(-j*w*6); %calculated H(w) of hamming
window

H_ham = abs(H_ham); %calculates magnitude
plot(w,H_ham), title('Hamming Window magnitude spectrum'),
xlabel('w'),ylabel('|H(w)|')
```

Output:

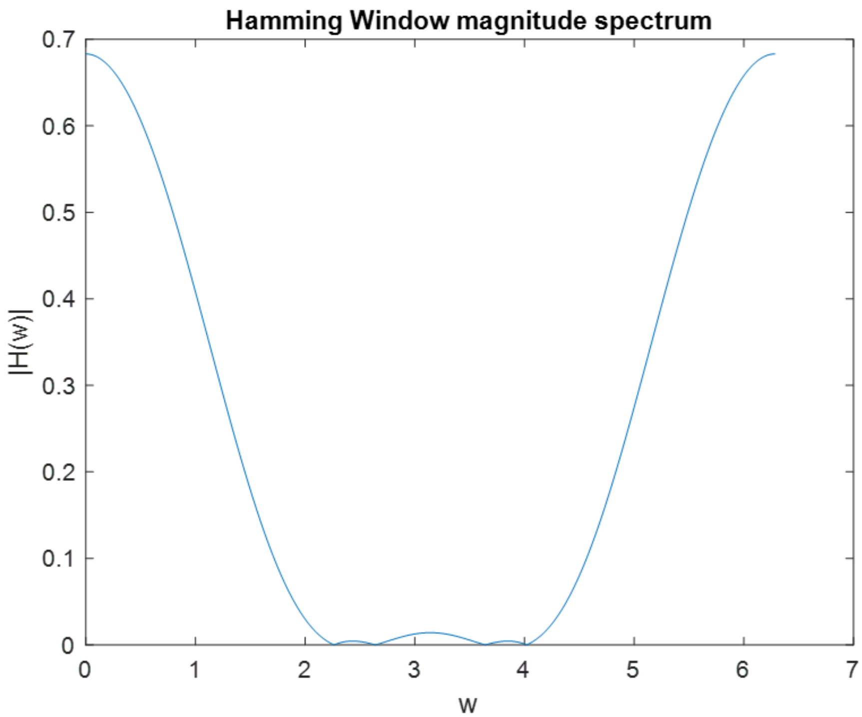

Fig 7: Magnitude Spectrum with Calculated values

Phase Spectrum:

Code:

```
clc
clear all
close all

w = 0: 0.001: 2*pi;
H_ham = -0.006*exp(-j*w*0) + 0.04929*exp(-j*w*1) +
0.17325*exp(-j*w*2) + 0.25*exp(-j*w*3) + 0.17325*exp(-j*w*4)
+0.04929*exp(-j*w*5) -0.006*exp(-j*w*6); %calculated H(w) of hamming
window

ph_ham = angle(H_ham); %calculates phase
plot(w,ph_ham), title('Hamming Window Phase spectrum'),
xlabel('w'),ylabel('<H(w)')
```

Output:

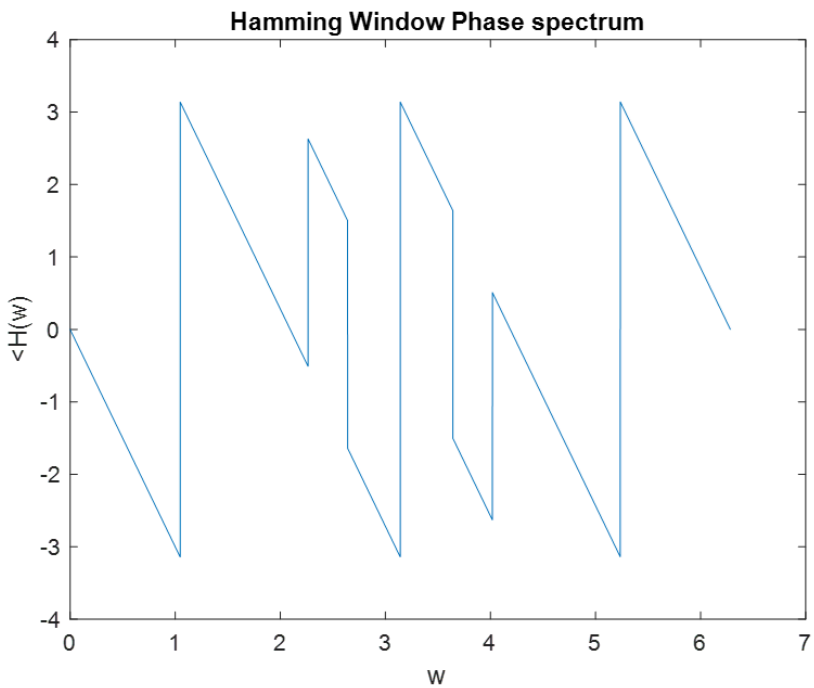

Fig 8: Phase Spectrum with Calculated values

Default Function:

Code:

```
clc
clear all
close all

a_ham = -fir1(6, 3/4, hamming(7))%finds h'(n) coefficients
fvtool(a_ham) %plots magnitude spectrum
```

Output:

```
Command Window

a_ham =

   -0.0059    0.0489   -0.1716   -0.7426   -0.1716    0.0489   -0.0059

fx >>
```

Fig 9: H’(n) coefficients with default matlab function

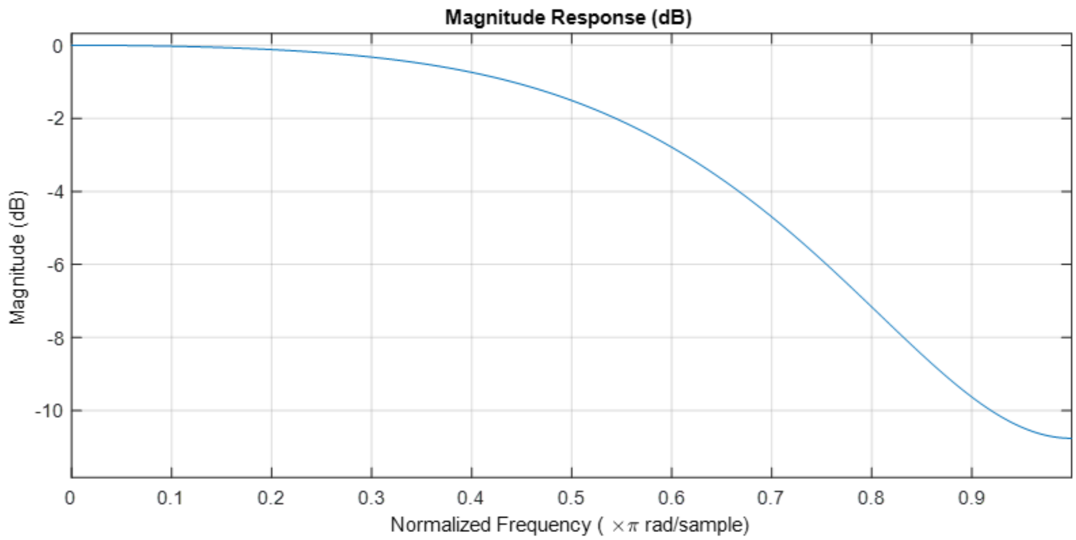

Fig 10: Magnitude Spectrum with default matlab function

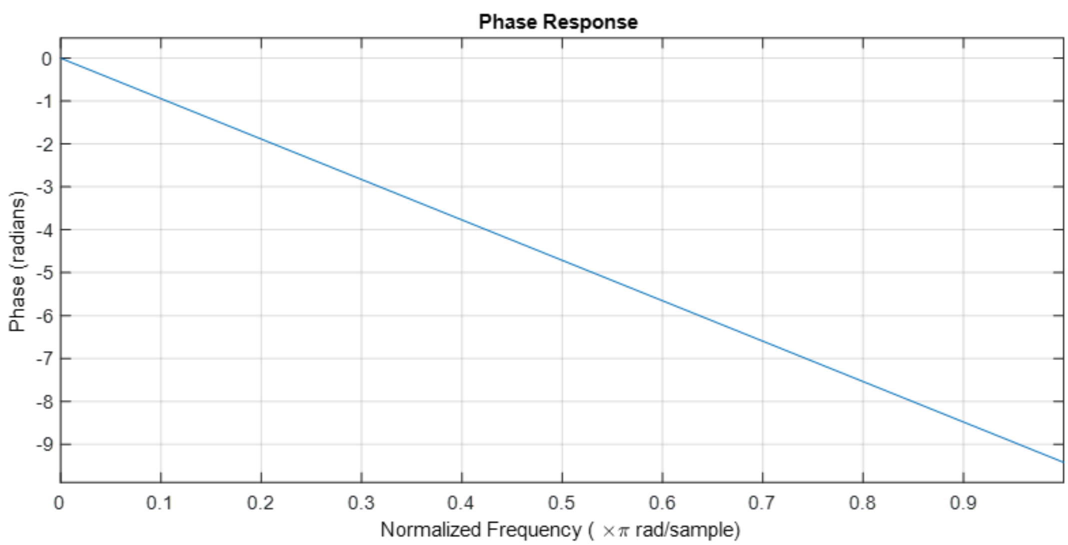

Fig 11: Phase Spectrum with default matlab function

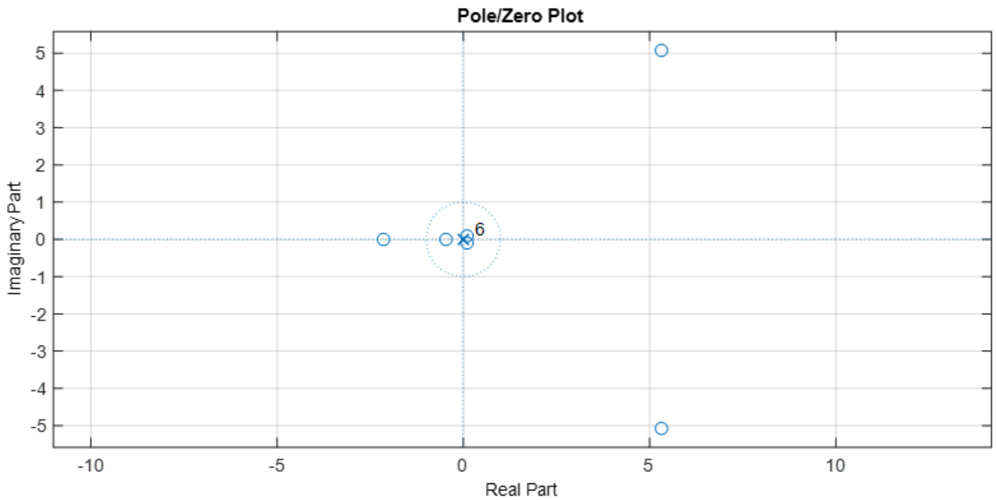

Fig 12: Pole zero plot with default matlab function

Hanning Window:

Magnitude Spectrum:

Code:

```
clc
clear all
close all

w = 0: 0.001: 2*pi;
H_han = 0*exp(-j*w*0) + 0.03975*exp(-j*w*1) - 0.16875*exp(-j*w*2) +
0.25*exp(-j*w*3) - 0.16875*exp(-j*w*4) + 0.03975*exp(-j*w*5) +
0*exp(-j*w*6);%calculated H(w) of hanning window

H_han = abs(H_han);%calculates magnitude
plot(w,H_han), title('Hanning Window magnitude spectrum'),
xlabel('w'),ylabel('|H(w)|')
```

Output:

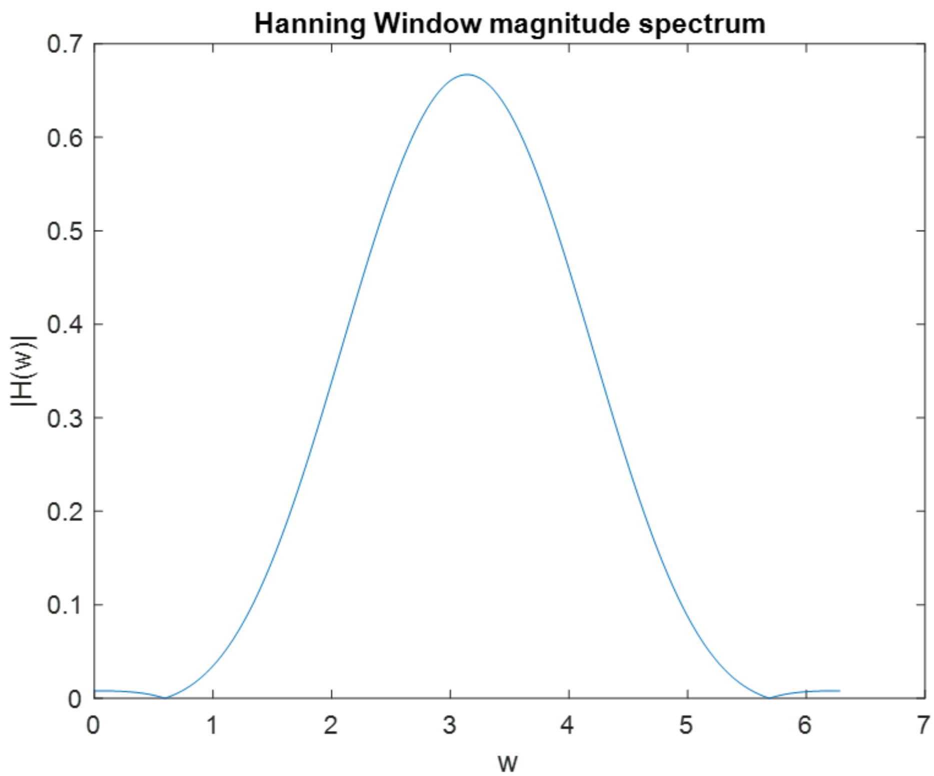

Fig 13: Magnitude Spectrum with Calculated values

Phase Spectrum:

Code:

```
clc
clear all
close all

w = 0: 0.001: 2*pi;
H_han = 0*exp(-j*w*0) + 0.03975*exp(-j*w*1) - 0.16875*exp(-j*w*2) +
0.25*exp(-j*w*3) - 0.16875*exp(-j*w*4) + 0.03975*exp(-j*w*5) +
0*exp(-j*w*6);%calculated H(w) of hanning window

ph_han = angle(H_han);%calculates phase
plot(w,ph_han), title('Hanning Window Phase spectrum'),
xlabel('w'),ylabel('<H(w)')
```

Output:

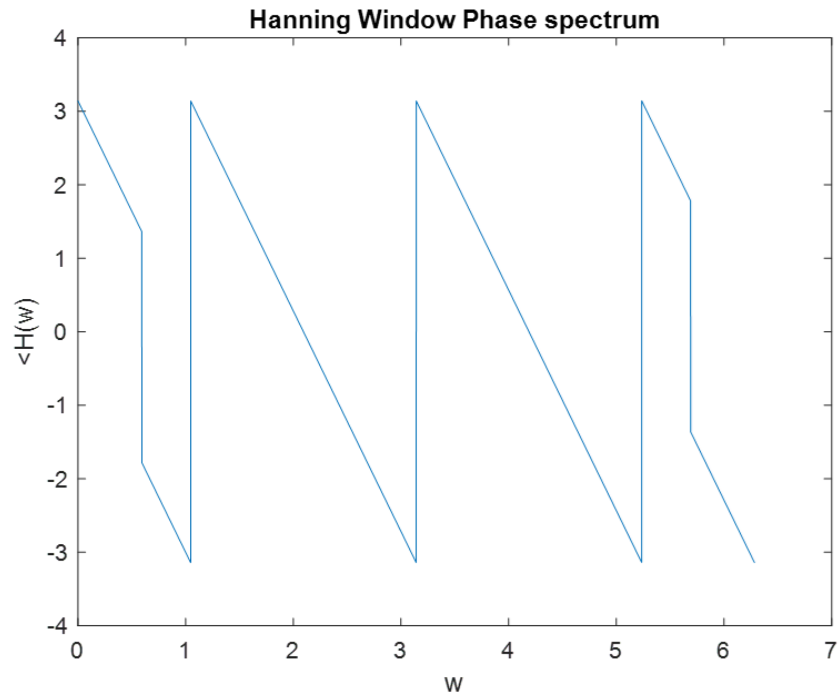

Fig 14: Phase Spectrum with Calculated values

Default Function:

Code:

```
clc
clear all
close all

a_han = -fir1(6, 3/4, hann(7))%finds h'(n) coefficients
fvtool(a_han) %plots magnitude spectrum
```

Output:

```
Command Window

a_han =

         0    0.0395   -0.1675   -0.7440   -0.1675    0.0395         0

fx >>
```

Fig 15: H'(n) coefficients with default matlab function

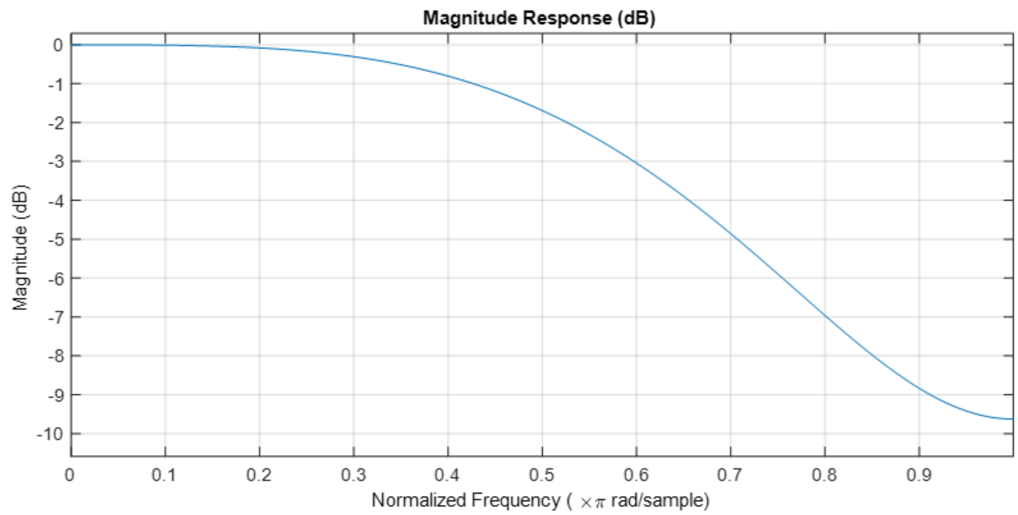

Fig 16: Magnitude Spectrum with default matlab function

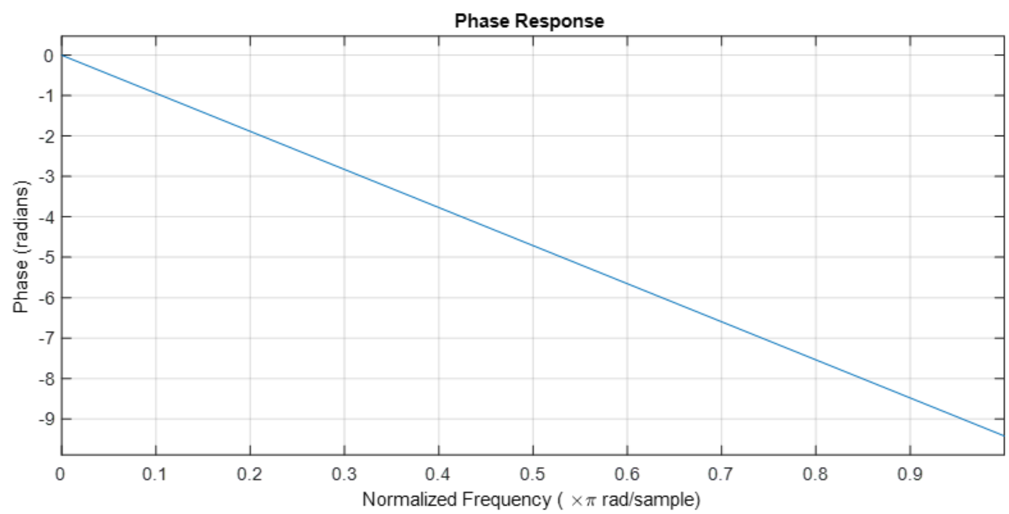

Fig17: Phase Spectrum with default matlab function

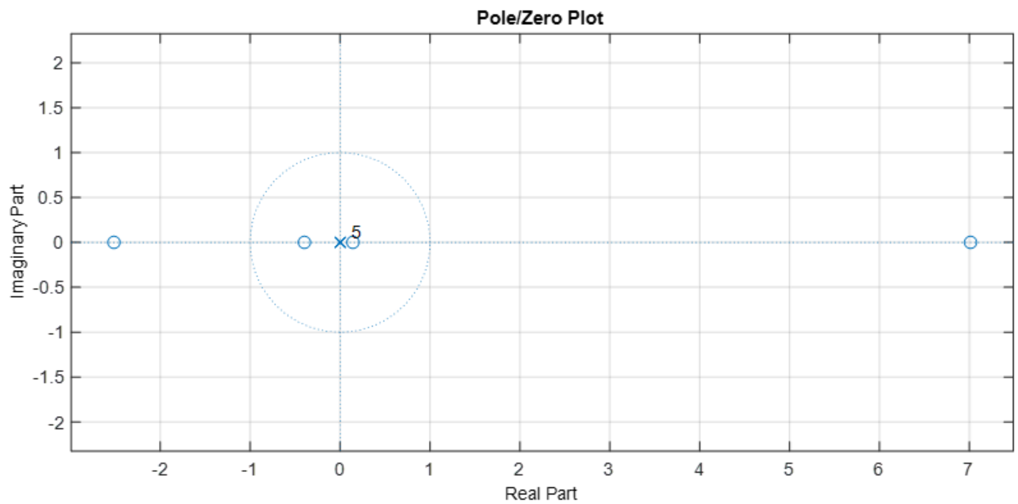

Fig 18: Pole Zero plot with default matlab function

Comparison And Analysis:

Frequency Analysis:

As we can see in the plots of calculated values, both magnitude and phase spectrum both have axes in with normal coefficients whereas with the default matlab function, both magnitude and phase spectrum is given in dB. If we could change calculated plots in dB, we could have analyzed that both the plots are very similar to each other. In the x-axis of default plots, normalized frequency is multiplied by pi, which is default by matlab and cannot be changed. With furthermore evaluation, we see that the graph's hamming window shows linear output, compared to the other two windows.

Filter Coefficients:

With my calculations (Handwritten part) and default matlab functions, we can see that both h(n) and h'(n) are almost identical. All the values from n = 0 to n = 6, the coefficient values match, except at n = 3. As matlab has a default function, it somehow manipulates the value of n = 3, where it is supposed to be infinity. According to my hand calculations, I had to calculate the h(n) value at n = 3, with a different procedure whereas other values such as; n = 0,1,2,4,5,6 were calculated from the normal h(n) calculated equation. Therefore, if we could give some different input in matlab, then all of the values would be similar. However, in my case, I could see by comparing all the calculated values and matlab output, Hamming window's coefficients seem to be the closest and hence proving to give the closest results.

Stability:
By the help of pole-zero plots, we can clearly see that all of them are in marginally stable condition. This is because the filter plots do not have poles that can lie outside the unit circle, they only have zeros.

Conclusion:
In conclusion, the design and comparison of 7th order FIR filters using Rectangular, Hamming, and Hanning windows highlight importance in filter design regarding spectral performance and practical application. With all my calculations and the default matlab code's outputs, even though it is not that much evident but the given results and comparison analysis shows that, Hamming window is the most optimal window.

Drive link MATLAB Codes:
https://drive.google.com/drive/folders/1s2b34gnXlQeL1whHU8K8bsCcoc_pvSQ1?usp=sharing

BRAC UNIVERSITY

Inspiring Excellence

Department of Electrical and Electronic Engineering

Semester: Spring 2024

Course Code: EEE343/ECE343

Course Title: Digital Signal Processing

Section: 01

Literature Review Topic: Brain-Computer Interfaces; exploring background, current used methods and future advancements.

Name: Afrida Islam

ID: 21221030

A Literature Review on: Brain-Computer Interfaces; exploring background, current used methods and future advancements.

Afrida Islam[1]

1Department of Electrical and Electronics Engineering, BRAC University, Dhaka, Bangladesh

Article Info

Article history:

4 April, 2024

Keywords:

Electroencephalogram (EEG)

Brain Computer Interface

Feature extraction

Classification Algorithm

Signal Acquisition

PROBLEM STATEMENT

For this study, the problem statement centers around the difficulties associated with reliable and effective decoding of brain signals for brain computer interferences (BCI). Although research on Brain-Computer interfaces technology has been going for a very long time, there are still challenges in accurately understanding and deciphering the complex brain signals which hinders the smooth functioning with external devices. Not only complex neural signals but also these obstacles include noise and distortion susceptibility, variation of inter-subject patterns and also poor signal determination.

1. Introduction:

The direct relationship between the brain's electrical activity and the computer has achieved considerable attention for a very long time. Over the past 15 years, BCI research has been productively and fastly growing in fields of neuroscience study and development [1 2]. Brain-Computer interfaces, can be also termed as Brain-Machine Interfaces (BMI) helps users to communicate through brain signals without involving any muscular and peripheral neural activity. In simple words, the sensors attached to the brain capture electrophysiological (EEG) signals which are transmitted between the brain's neurons and transfer that signal to a device that can be attached externally, whether to a computer or robotic limb, this allows it to convert the user's thoughts into actions. Digital signal processing (DSP) plays an important role in the functioning of brain-computer interfaces. The key aspects of DSP such as: signal processing, decoding, feature extraction, classification and feedback [2] .

Recent studies have shown that BCI has transformed numerous fields of study and is quickly spreading in healthcare, study environments, neuroscience and also many studies are underway to improve its usage in medical science. BCI features offers help to many with severe motor disabilities such as amyotrophic lateral sclerosis (ALS), spinal cord injury, stroke and as well serving as a valuable machine for the patients with Parkinson's disease or traumatic brain injuries [8]. Beyond these applications, latest BCI research shows it has various uses in clinical and nonclinical fields.

Despite all these advancements, incorporating modern technology in usable and practical applications has always been a challenge and BCI is no exception. Some of the main factors that hamper BCI operation are the type of brain signals used as data, data collecting techniques, algorithms used, user control hardware and feedback the user gets after giving commands [6].

In this literature review, we aim to overview BCI, the state-of-the-art DSP techniques in BCI, as well as highlighting the potential of using BCI technology in different fields, also the challenges & limitations faced in this field and lastly outlining the future BCI development that may shape the field.

2. Background and Fundamentals:

Understanding the fundamentals of brain signals and digital signal processing, it is essential to learn about the complexities of BCI technology. In 1929, Hans Berger was the first person to record Electroencephalogram (EEG), following that in 1973, Vidal made the first effort to communicate between brain and computer [3] . Over time, BCI classification traditionally has been partitioned according to their classification: dependent or independent, invasive or non-invasive, exogenous or endogenous (figure 1) [5 6]. On dependable BCI, the user needs to specifically think about tasks or respond to generate detectable signals whereas on independent BCI, it does not require external stimuli to detect brain signals. Again, with invasive type, it involves implantation of electrodes or sensors directly into the brain tissue (mostly used in medical appliances), showcasing differently, with non-invasive type, it does not require surgical methods, it relies on external activity. Lastly, on exogenous BCI, the brain signals are transmitted manually from the users to predefined stimuli by the BCI, whereas on endogenous BCI, the user produces signals from the brain without any predefined given prompt by BCI.

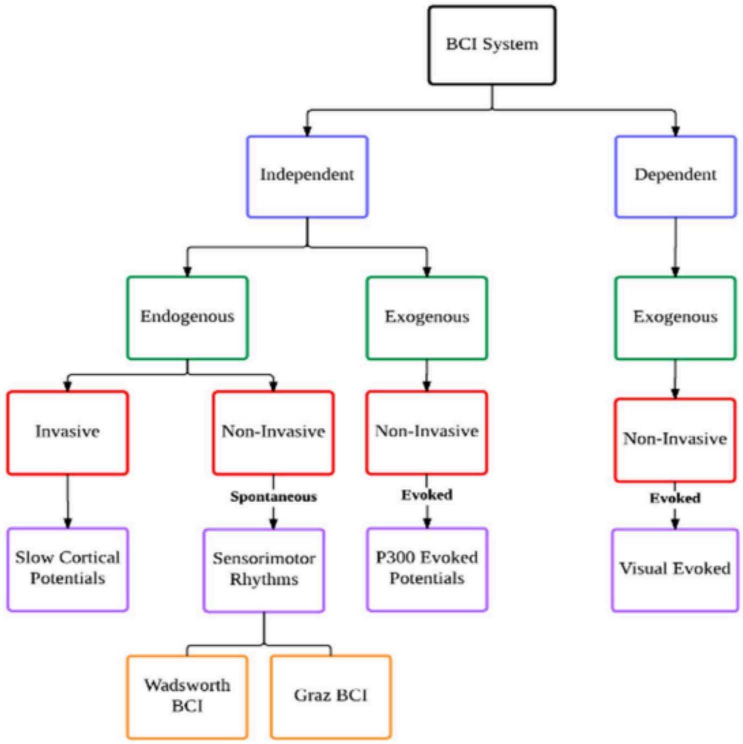

Figure 1: Abstract classification of BCI development

On the other hand, direct brain-to-computer signal amplification is the backbone of brain computer interference. Even though some of the signals are easy to extract but mostly are more complex and need preprocessing. Of these, the control signals can be summarized in three categories: evoked signal, spontaneous signal and hybrid signals (Figure 2) [3].

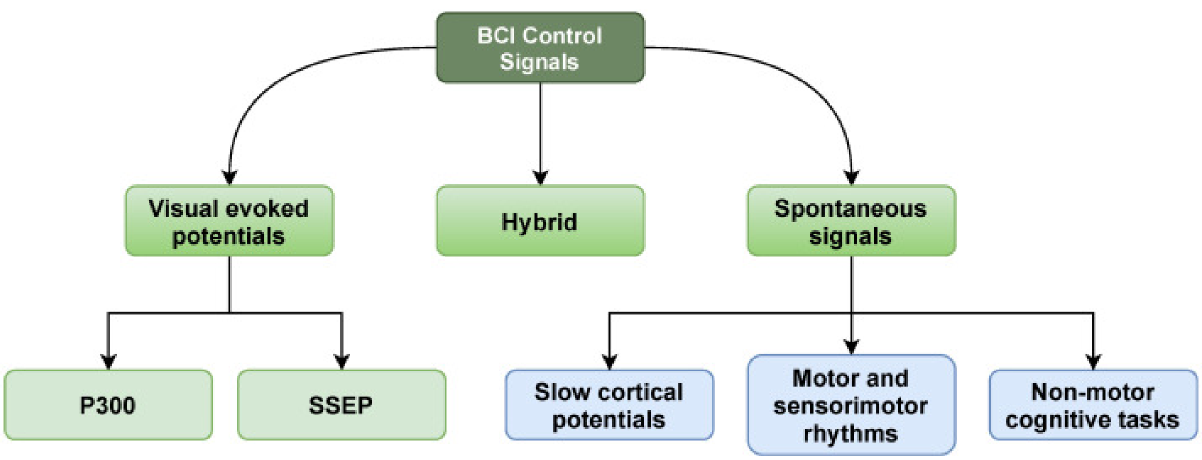

Figure 2: Basic flowchart of BCI control signals

In recent times, most popular and effective systems are based on non-invasive BCI systems. Most of the electroencephalogram (EEG) based BCI system relies on auditory steady-state response (ASD), steady-state visual evoked potentials (SSVEP), slow cortical potentials (SCP), sensorimotor oscillations (SMR), and various hybrid systems (based on more than one input signal) are associated with motor imagery (MI) [7].

This section provides an overview about the background of brain computer interferences, classification of BCI system, signal amplification of BCI control system and as well the most effective system analysis based on recent research and work.

3. Methodology And Techniques:

The working principle of BCI requires three units: signal acquisition module, signal processing and application module. This section provides a brief overview of these modules and shows the components of BCI (figure 3) with their interconnections [4 5].

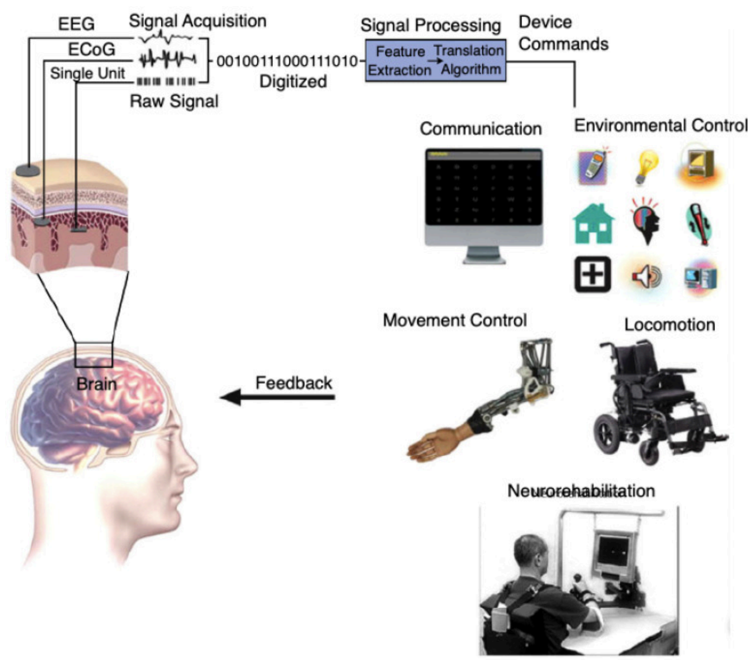

Figure 3: Components of BCI system

3.1 Signal Acquisition Module:

The electrophysiological signals from the brain that provide input to BCI are recorded in the signal acquisition module. The aim of signal analysis is to maximize the signal-to-noise ratio (SNR) of the EEG or single-unit features- which conveys the user's message [5]. Here Electrocardiograms (ECoG) and single-neuron recordings are examples of invasive techniques which can produce higher quality signals whereas non invasive methods contains Near-Infrared Spectroscopy (NIRs), Functional Magnetic Resonance Imaging (fMRI), Electroencephalogram (EEG), Magnetoencephalogram (MEG), and Positron Emission Tomography (PET) [4].

3.2 Signal processing Module:

The signal processing methodology flow is divided into three simultaneous steps: preprocessing, feature extraction and classification. In preprocessing, the recorded signals are enhanced by signal-to-noise ratio (SNR). In BCI, signal preprocessing is based on the Covariance Matrix Adaptation Evolution Strategy (CMA-ES) that basically determines the structural and frequency adopting filters. After signal preprocessing, the signal is getting inputted into one or multiple feature extraction (figure 4). There are certain methods of feature extractions including Fast fourier transform (FFT), Autoregressive (AR) model, Wavelet transform (WT), Common spatial pattern (CSP). The objective of classification is to convert the independent variable into dependable by categorizing the characteristic produced by feature extraction.

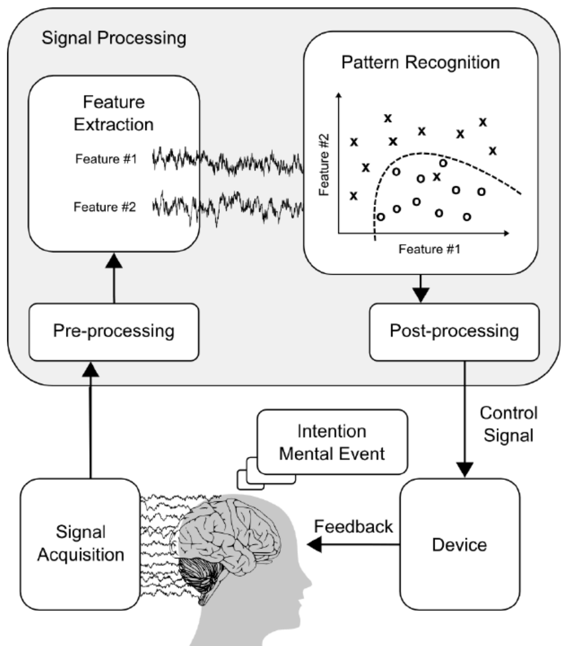

Figure 4: Feature extraction

3.3 Application Module:

The device output is the general outcome component of the Brain Computer Interface system. A closed loop feedback occurs when the consumer extracts output from the initial operating system of the device. The most current BCI technology uses a computer screen as the output device. Other output devices can be frequently used to move a cursor on a computer screen, operate a robotic arm, control a wheelchair or other assistive technology, or allow movement of a paralyzed limb via the use of a neuroprosthesis [8].

4. State of the Art:

Modern BCI is classified into five classes: VEPs, slow cortical potentials, P300 evoked potentials, mu and beta rhythms (sensorimotor rhythms), and neuronal action potentials. They can be identified as per the brain impulses from the user [6]. Researchers have studied vastly in the field of signal processing to identify the key advancement factors for Brain Computer Interface (BCI). As the latest study of BCI includes better accuracy, it is able to create a better algorithm of brain signals. Which provides a better understanding on controlling external devices through brain activities. The growing idea about this field gives the significance of electroencephalography (EEG) and functional near-infrared spectroscopy (fNIRS), that offers a remarkable result in overall accessibility, brain information processing and further communication [7].

Even though brain computer interference is advancing towards a more dynamic and accuration connection between brain and computer, there are still few factors resisting the main goal. The first issue is the slower transfer rate of signals, increasing it would make a significant change. Again, issues lie in training time for the user to get used to it as well Psychophysiological and Neurological Challenges. And lastly, some ethical challenges including physical, psychological and social factors [3 6 8].

5. **Critical Analysis and Comparison:**

Critical Analysis and comparison of various approaches and methods of Brain-Computer interference relies on the efficacy, dependability and viability in enabling direct communication between brain and computer. The breakdown for the critical analysis and comparison of each of the methods discussed in the literature with their respective strength, weakness and gap is discussed below.

Approach/Method	Strengths	Weaknesses	Gaps	Reference
Feature extraction Techniques	Accurate at frequency composition and resolution	Not suitable for non-linear signals and takes time	Need to handle noisy and complex brain signals more effectively	[4]
Classification Algorithm	Low computation, simple to use	Not suitable for non-linear EEG data and handling dynamic nature	Need to develop Machine Learning models with more accuracy	[4]
Feedback Mechanism	Real-time results	Adds distraction to user	Need personalized feedback	[4]

Table 1: Comparison Analysis of different signal processing and application methods.

6. Future Directions:

The future goal of BCI system research is to overcome existing constraints and move the field closer to more useful applications. It will continue to expand its field of application into the development of advanced research and as well treatment, diagnostic, and assistive technology. Even though BCI technology has proven to be reliable and effective, it is still limited to research only. Despite all the published research and papers, BCI is still only on papers and lacks experimental data from any clinical trial. Furthermore, if non-invasive BCI systems with several independent controls such as: multiple dimension control of neural prosthetics or mixed signals are further developed, BCI applications will grow more. This will enable users to carry out difficult activities smoothly and easily [8].

In addition, all the paper works and research shows direct brain to external world communication is feasible and can serve many useful purposes. But at the same time practicality does not match fantasy. With only the scientists, medical professionals and tech sector working all together will bring revolutionary change in BCI, by making it commercially available and as well accessible to the general public[1 2 8] .

7. Conclusion:

As years passed and technological advancements took place, the general advancement of research in BCI showed remarkable results and promising outcomes. The following literature review highlights the BCI functionality, addressing signal processing, decoding, feature extraction and feedback algorithms. The study of multiple resources provided a major insight and guide work of how Digital signal processing and the extraction of EEG signals contributes to the advancements of technologies correlated to BCI. The scope of BCI spreads beyond its study, as it shows its flexible applicability in education field, medical field, neurological researches and even more. Despite the challenges of digital signal processing, BCI stands with immense potential to revolutionize machine learning strategies, as well as human-machine interaction to enhance the way of living.

References:

1. Wolpaw, J. R., Birbaumer, N., McFarland, D. J., Pfurtscheller, G., & Vaughan, T. M. (2002). Brain–computer interfaces for communication and control. *Clinical Neurophysiology*, *113*(6), 767–791. https://doi.org/10.1016/s1388-2457(02)00057-3
2. Wolpaw, J. R. (2013). Brain–computer interfaces. In *Handbook of clinical neurology (Print)* (pp. 67–74). https://doi.org/10.1016/b978-0-444-52901-5.00006-x
3. Mridha, M. F., et al. "Brain-Computer Interface: Advancement and Challenges." *Sensors*, vol. 21, no. 17, 26 Aug. 2021, p. 5746, https://www.ncbi.nlm.nih.gov/pmc/articles/PMC8433803/
4. Aggarwal, S., & Chugh, N. (2019). Signal processing techniques for motor imagery brain computer interface: A review. *Array*, *1–2*, 100003. https://doi.org/10.1016/j.array.2019.100003
5. *Brain-Computer Interface Technology: A Review of the First International Meeting*, www.researchgate.net/publication/12423403_Brain-Computer_interface_technology_A_review_of_the_first_international_meeting. Accessed 3 Apr. 2024.
6. An overview of brain computer interfaces. (n.d.). https://www.cse.unr.edu/~fredh/papers/conf/144-aoobci/paper.pdf
7. Kawala-Sterniuk, Aleksandra, et al. "Summary of over Fifty Years with Brain-Computer Interfaces—a Review." *Brain Sciences*, vol. 11, no. 1, 3 Jan. 2021, p. 43, https://doi.org/10.3390/brainsci11010043.
8. Alkaff, Z. A., Malim, N. H. a. H., Sumari, P., & Abdullah, J. M. (2024). Applications of brain computer interface in present healthcare setting. In *Artificial intelligence*. https://doi.org/10.5772/intechopen.112353

BIBLIOGRAPHY OF AUTHORS

Afrida Islam is an undergraduate student, currently studying in BRAC University on Electrical & Electronics Engineering. Her research and study focuses on development of the upcoming world's technology based study. Such as, study of EEG signals and BCI. She reflects a promising effort and result in this field & wishes to expand this knowledge even wider.

Contact with **Afrida** at afrida.islam@g.bracu.ac.bd